

Synthesis and Characterization of a Novel Chiral Molecular-Based Ferrimagnet Prepared from a Chiral Nitronyl Nitroxide Radical and Manganese(II) Ion

Motoko Akita-Tanaka,[†] Hitoshi Kumagai,^{††} Ashot Markosyan,^{†††} and Katsuya Inoue^{*,†}

Institute for Molecular Science, 38 Nishigounaka, Myoudaiji, Okazaki 444-8585

Received February 28, 2006; E-mail: kxi@hiroshima-u.ac.jp

A new chiral organic radical, 4,4,5,5-tetramethyl-2-{4-[(*S*)-2-methylbutoxy]phenyl}-3-oxido-4,5-dihydroimidazol-1-oxyl (**1**) and its Mn^{II} complex ([**1**·Mn^{II}(hfac)₂]_n) (hfac = hexafluoroacetylacetonato) were synthesized and characterized. From single crystal X-ray structure analysis, **1** and [**1**·Mn^{II}(hfac)₂]_n have a chiral space group (*P*2₁2₁2₁), and [**1**·Mn^{II}(hfac)₂]_n has a one-dimensional helical structure. Magnetic susceptibility measurements of [**1**·Mn^{II}(hfac)₂]_n indicate that this heterospin system behaves as a ferrimagnet with very weak interchain ferromagnetic exchange interaction.

There has been considerable interest in synthesizing organic–inorganic hybrid materials due to their intriguing structural diversity and potential dual or multiple functions, such as superconductivity, non-linear optical activity, and magnetism.^{1–5} Rational synthesis of 1D-, 2D-, and 3D-coordination network with appropriate bridging ligands is fundamental in developing these materials. A strategy using π -conjugated polyaminooxyl radicals with high-spin ground states as bridging ligands for magnetic metal ions to assemble and align the electron spins on a macroscopic scale has been reported.^{6–8} The crystal structures and magnetic structures of these complexes can be tuned using this strategy.⁹ The majority of these materials are based on achiral organic radicals and the resulting complexes form achiral crystals. We have reported the crystal structure and magnetic properties of Mn^{II} complex made up of a chiral diradical.¹⁰ The synthesis and study of chiral molecule-based magnets, which are transparent to light, are of great interest.^{3,11–13} Although novel properties are expected for such compounds, few examples are still known.^{14,15} To expand our chemistry, we designed and synthesized a new chiral organic radical, 4,4,5,5-tetramethyl-2-{4-[(*S*)-2-methylbutoxy]phenyl}-3-oxido-4,5-dihydroimidazol-1-oxyl (**1**), which can be used to construct chiral molecule-based magnets. This work concerns with synthesis and characterization of a novel 1D chiral complex made up of new chiral organic radical **1** and Mn^{II} ion.

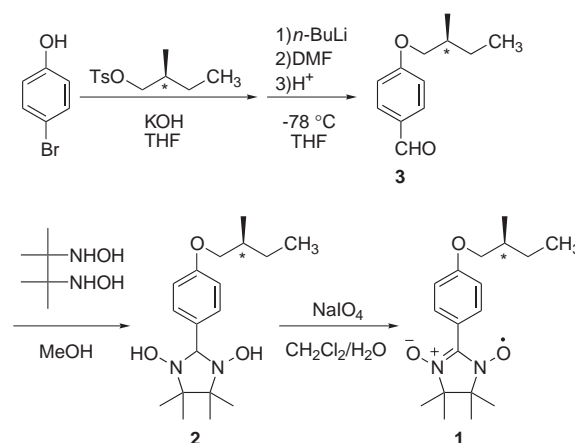
Experimental

All chemicals were obtained from Wako and Tokyo Kasei Co., Ltd. and used without purification. Solvents were distilled under nitrogen atmosphere before use. Infrared spectra were recorded

on a Perkin-Elmer Spectrum BX FT-IR system with the samples as KBr pellets. The temperature and field dependence of the magnetization of the complex were performed on a Quantum Design MPMS-5S SQUID operating in the temperature range of 2–300 K and fields up to 5 Tesla. AC measurements were performed in frequency range of 1–10 Hz with AC field amplitude of 3 Oe.

Preparation. The synthetic route to prepare radical **1** is illustrated in Scheme 1. Compound **2**: *N,N'*-2,3-dimethylbutane-2,3-diylbis(hydroxylamine) was condensed with *p*-[(*S*)-2-methylbutoxy]benzaldehyde (**3**) in methanol. Mp 147.2–150.9 °C, MS (*m/z* = 322), HRMS *m/z* found 322.2247 calcd for C₁₈H₃₀N₂O₃ 322.2256, ¹H NMR (270 MHz, CDCl₃) δ 7.40 (d, 2H), 6.88 (d, 2H), 4.90 (brs, 2H), 4.70 (s, 1H), 3.9–3.6 (m, 2H), 1.95–1.75 (m, 1H), 1.4–1.2 (m, 2H), 1.16 (s, 12H), 1.02 (s, 3H), 0.94 (s, 3H).

Compound **1**: Compound **2** was oxidized with NaIO₄/water in dichloromethane at 0 °C and purified by column chromatography on silica gel eluted with ether. Mp 84.2 °C, MS (*m/z* = 319), HRMS *m/z* found 319.2006 calcd for C₁₈H₂₇N₂O₃ 319.2022, EPR (9.4522 GHz, hexane) *g* = 2.0058, *a_N* = 7.63 G; UV–vis (hexane) $\lambda_{\max}(\epsilon)$ 297 (8180) nm, 366 (9900) nm, 634 (550) nm, [α]_D²⁰ = 323° (*c* 0.0124, hexane). μ_B value (300 K) 1.74 μ_B .



Scheme 1.

[†] Present address: Graduate School of Science, Hiroshima University, 1-3-1 Kagamiyama, Higashi-Hiroshima 739-8526

^{††} Present address: Toyota Central R&D Labs. Inc., 41-1 Yokomichi, Nagakute, Aichi-gun, Aichi 480-1131

^{†††} Present address: M.V. Lomonosov Moscow State University, 119899 Moscow, Russia

Preparation of $[1 \cdot \text{Mn}^{\text{II}}(\text{hfac})_2]_n$. Chiral radical **1** was mixed with an equimolar amount of dehydrated $\text{Mn}(\text{hfac})_2$ in diethyl ether/heptane. The mixture was evaporated to ca. 10 mL and green block crystals were obtained at -30°C within 1 week. Mp $141.6\text{--}143.6^\circ\text{C}$ (decomp.), Anal. Found: C, 42.19; H, 3.37; N, 3.47%, Calcd for $\text{C}_{28}\text{H}_{29}\text{F}_{12}\text{MnN}_2\text{O}_7$: C, 42.65; H, 3.71; N, 3.55%, EPR (9.4522 GHz, polycrystalline sample) $g = 2.0100$, UV-vis (hexane) $\lambda_{\text{max}}(\epsilon)$ 300 (13600) nm, 366 (5200) nm, 635 (1100) nm, $[\alpha]_{\text{D}}^{30} = 1890^\circ$ (c 0.0200, hexane).

X-ray Crystallography and Structure Solution. Selected single crystals were glued on the tip of glass fibers. The diffractometer is equipped with a graphite monochromated $\text{Mo K}\alpha$ (0.7107 Å) radiation. The data were corrected for Lorentz and polarization effects. The structure was solved by direct methods and expanded using Fourier techniques. The non-hydrogen atoms were refined anisotropically. Hydrogen atoms were placed at the calculated ideal positions. The final cycle of full-matrix least-squares refinement was based on the number of observed reflections and n variable parameters. They converged (large parameter shift was σ times its e.s.d.) with agreement factors of $R = \Sigma||F_o| - |F_c||/\Sigma|F_o|$, $R_w = [\Sigma w(|F_o| - |F_c|)^2/\Sigma w|F_o|^2]^{1/2}$. No extinction corrections were applied.

X-ray structure analysis for **1**: Reflection intensities were measured at -100°C on a Rigaku RAXIS-IV imaging plate area detector. Crystal data for **1**: $\text{C}_{18}\text{H}_{27}\text{N}_2\text{O}_3$, $M_w = 319.43$, crystal size, $0.20 \times 0.10 \times 0.05 \text{ mm}^3$; Orthorhombic, $a = 11.494(3) \text{ Å}$, $b = 25.328(3) \text{ Å}$, $c = 6.1281(5) \text{ Å}$, $V = 1748.0(4) \text{ Å}^3$, Space group $P2_12_12_1$ (No. 19), $Z = 4$, $D_{\text{calcd}} = 1.189 \text{ g cm}^{-3}$, absorption coefficient, 0.81 cm^{-1} ; Reflections, 1389 ($I > 2.00\sigma(I)$); R (R_w) = 0.067 (0.083), parameters, 208; maximum and minimum residual electron densities, $0.30 \text{ e}^-/\text{Å}^3$ and $-0.41 \text{ e}^-/\text{Å}^3$, respectively. The crystal data have been deposited at CCDC, Cambridge, UK and given the reference numbers CCDC 284812.

X-ray structure analysis for $[1 \cdot \text{Mn}^{\text{II}}(\text{hfac})_2]_n$: Reflection intensities were measured at 25°C with ω scan mode on a Bruker SMART CCD diffractometer. Crystal data for complex $[1 \cdot \text{Mn}^{\text{II}}(\text{hfac})_2]_n$: $\text{C}_{28}\text{H}_{29}\text{F}_{12}\text{MnN}_2\text{O}_7$, $M_w = 788.47$, crystal size, $0.46 \times 0.23 \times 0.22 \text{ mm}^3$; Orthorhombic, $a = 14.081(1) \text{ Å}$, $b = 15.940(1) \text{ Å}$, $c = 16.075(1) \text{ Å}$, $V = 3608.1(4) \text{ Å}^3$, Space group $P2_12_12_1$ (No. 19), $Z = 4$, $D_{\text{calcd}} = 1.452 \text{ g cm}^{-3}$, absorption coefficient, 4.71 cm^{-1} ; Reflections, 8695 ($I > 2.00\sigma(I)$); $R1$ ($wR2$) = 0.0690 (0.1692). Absolute structure parameter, $-0.03(3)$; parameters, 451; maximum and minimum residual electron densities, $0.477 \text{ e}^-/\text{Å}^3$ and $-0.393 \text{ e}^-/\text{Å}^3$, respectively. The crystal data have been deposited at CCDC, Cambridge, UK and given the reference numbers CCDC 284813. Copies of the data can be obtained free of charge via <http://www.ccdc.cam.ac.uk/conts/retrieving.html> (or from the Cambridge Crystallographic Data Centre, 12, Union Road, Cambridge, CB2 1EZ, UK; Fax: +44 1223 336033; e-mail: deposit@ccdc.cam.ac.uk).

Results and Discussion

From the X-ray crystal structure analysis, both **1** and $[1 \cdot \text{Mn}^{\text{II}}(\text{hfac})_2]_n$ crystallize in the same chiral space group $P2_12_12_1$ (No. 19). The molecular structure of $[1 \cdot \text{Mn}^{\text{II}}(\text{hfac})_2]_n$ is depicted in Fig. 1. The asymmetric unit of $[1 \cdot \text{Mn}^{\text{II}}(\text{hfac})_2]_n$ consists of one Mn^{II} ion, two hfac anions, and one chiral radical **1**. The Mn^{II} ion has an octahedral coordination environment with four oxygen atoms of two hfac anions and two oxygen atoms of different nitronyl nitroxide molecules. As the result, Mn^{II} and **1** form a 1D chain along the a -axis. The shortest

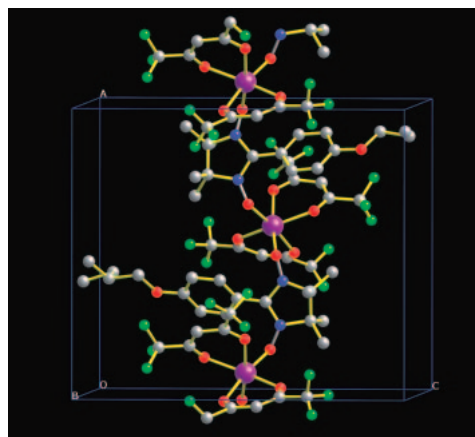


Fig. 1. A view of the helical chain formed by the chiral nitronyl nitroxide **1** and $\text{Mn}^{\text{II}}(\text{hfac})_2$. Hydrogen atoms are omitted for clarity.

interchain contact between the Mn^{II} ion and the oxygen atom of **1** is 9.2 Å , while the shortest $\text{Mn}^{\text{II}}\text{--Mn}^{\text{II}}$ interchain distance is 10.7 Å . The radicals are bound to a Mn^{II} ion in a *cis*-fashion to each other. A detailed description of the coordination sphere of Mn^{II} must take into account the possible configurations resulting from the *cis*-coordination arrangement, which can lead to Δ or Λ configurations. In this complex, the metal centers all exhibit a Δ configuration. The absolute configuration of a metal center is often affected by chirality of the organic ligand, and our results show a similar effect from the chiral carbon atom of **1**.¹⁰ Since no inversion centers are present in this space group, the chains are completely isotactic, and the crystal lattice as a whole is chiral. The UV-vis spectrum of $[1 \cdot \text{Mn}^{\text{II}}(\text{hfac})_2]_n$ were measured in hexane solution and the crystalline state in KBr disk. Both spectra exhibit absorption around 300, 365, and 635 nm. They are very similar to each other and different from that of the free radical **1**. This results indicate that the interaction between **1** and $\text{Mn}^{\text{II}}(\text{hfac})_2$ in the complex is retained in hexane. The solution of $[1 \cdot \text{Mn}^{\text{II}}(\text{hfac})_2]_n$ in hexane exhibits optical rotation, which indicates that $[1 \cdot \text{Mn}^{\text{II}}(\text{hfac})_2]_n$ is chiral in solution.

The temperature dependence of χT of a microcrystalline sample of $[1 \cdot \text{Mn}^{\text{II}}(\text{hfac})_2]_n$ is shown in Fig. 2. At 300 K, $\chi T = 5.11 \text{ emu K mol}^{-1}$, which is larger than the theoretical value ($4.75 \text{ emu K mol}^{-1}$) for isolated spins of organic radicals and Mn^{II} ions, and it increases monotonically with decreasing temperature. In the paramagnetic range, the complex was treated as a heterospin 1D ($\cdots -1/2 - 5/2 - \cdots$)-chain compound, and a fit to the experimental data was made using the Heisenberg quantum-classical approximation: $\mathcal{H} = J \Sigma (S_i + S_{i+1}) S_i$. For a quantum spin $1/2$ and a classical spin $5/2$, the expression for χT .

$$(\chi T)_{\text{Ch}} = \frac{N\mu_B^2}{3k} \left[38 + \frac{2}{1-P} (25P - 10Q + Q^2) \right] \quad (1)$$

where

$$P = 1 + 12\gamma^{-2} - 2 \frac{1 + 2 \cosh \gamma}{1 - \cosh \gamma + \gamma \sinh \gamma},$$

$$Q = \frac{\cosh \gamma}{\gamma^{-1} - \gamma^{-1} \cosh \gamma + \sinh \gamma} \quad \text{and} \quad \gamma = 2.5 \frac{J}{kT}.^{16}$$

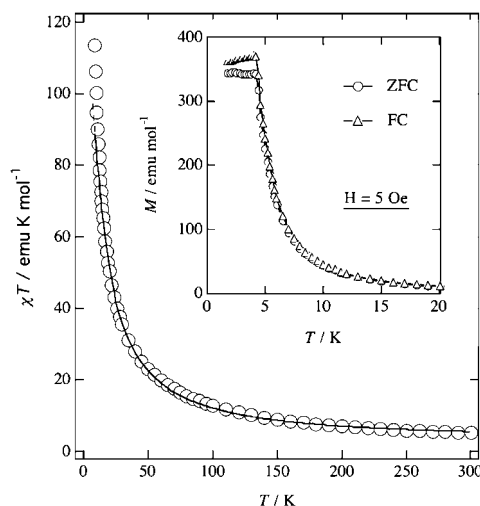


Fig. 2. The temperature dependence of the product χT for the complex $[1 \cdot \text{Mn}^{\text{II}}(\text{hfac})_2]_n$. The inset shows field-cooled (FC) and zero-field-cooled (ZFC) magnetization versus T plots.

A weak mean field correction was introduced in order to take into account the interchain exchange according to the expression $\chi T = [(\chi T)_{\text{Ch}}^{-1} - \lambda/T]^{-1}$ where λ refers to the interchain exchange. In Fig. 2, the solid line is the least squares fit of this equation to the experimental data in the range of 15–300 K. The fit parameters that were obtained are: $J/k = -435 \pm 5$ K and $\lambda' = (zJ'/k) = -0.0275 \pm 0.005$ K. J' is interchain magnetic exchange interaction parameter. If the number of nearest neighbors for a given chain $z = 4$, one obtains $J'/J = 1.5 \times 10^{-5}$. Hence, $[1 \cdot \text{Mn}^{\text{II}}(\text{hfac})_2]_n$ is characterized by low dimensionality along with a strong negative (ferrimagnetic) metal–radical exchange interaction.

The field-cooled (FC) and zero-field-cooled (ZFC) magnetizations were traced at a low field of 5 Oe over the temperature range from 1.8 to 20 K. The magnetization signal of both the traces decreased sharply with increasing temperature. The inset in Fig. 2 shows the difference between the two signals and points to a possible magnetic ordering at ca. 4.5 K. The magnetic measurements and X-ray crystal structure analysis both indicate that the interaction between the chains is expected to be ferromagnetic, making $[1 \cdot \text{Mn}^{\text{II}}(\text{hfac})_2]_n$ complex, which is an assembly of chiral one-dimensional chains, a molecule based ferrimagnet with $J'/k > 0$. AC susceptibility measurements also revealed a maximum of χ at $T_C \approx 4.5$ K, which is characteristic of a ferrimagnetic ordering. It should be noted that the J'/k value evaluated from the fit to the paramagnetic susceptibility data (Fig. 2) is negative. The positive interchain exchange interaction obtained from the low-temperature measurements can be ascribed to factors that were not included in the model: effects of thermal expansion and the contribution from the positive dipole–dipole interactions that are important at low temperatures as well as neglect of the next-nearest neighbor exchange interactions.

The magnetization curves in paramagnetic phase of $[1 \cdot \text{Mn}^{\text{II}}(\text{hfac})_2]_n$ at different temperatures are given in Fig. 3. They remain substantially nonlinear far above T_C . The solid lines in this figure are theoretical fits to the experimental data by using the Brillouin function, $g\mu_B S_u B_{S_u}(g\mu_B H/kT)$, where

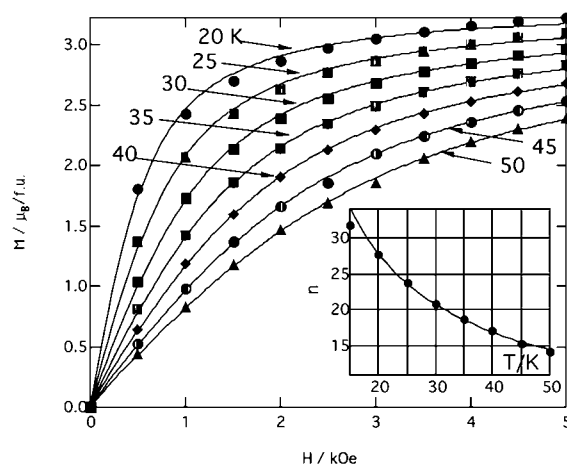


Fig. 3. The temperature dependence of the effective magnetic moment of $[1 \cdot \text{Mn}^{\text{II}}(\text{hfac})_2]_n$.

H is the external field and S_n is the unspecified spin value. In the fits of S_u , the value of the total spin per f.u. was $2\mu_B$. Hence S_n can be used to determine the average length the correlated spins make up at a given temperature. The inset in Fig. 3 shows the temperature variation of the number of the correlated units $n = S_n/S_u$. Down to 15 K, it can be approximated as $n = 1 + 250T^{-4/3}$.

In summary, a novel chiral nitronyl nitroxide radical and its Mn^{II} complex were prepared, and a chiral one-dimensional hybrid chain was realized. The complex has a helical-chain structure and is characterized by an (*S*) chiral carbon center along with a Δ configuration around the Mn^{II} ion. From magnetic susceptibility measurements, this chiral heterospin complex behaves as a ferrimagnetic one-dimensional chain system with an extremely low ratio between the intrachain and interchain exchange parameters ($J'/J = 1.5 \times 10^{-5}$).

We thank Prof. Dr. Hideaki Kanno in Shizuoka University for the measurement of optical rotation. We thank Dr. Kenji Yoza and Mr. Shinetsu Igarashi in Bruker Japan Co., Ltd. for the measurement of X-ray crystallography. This research was supported by a Grant-in-Aid for scientific research from the Ministry of Education, Culture, Sports, Science and Technology. We thank JSPS for the postdoctoral fellowship given to H.K.

References

- 1 P. G. Lacroix, R. Clement, K. Nakatani, J. Zyss, I. Ledoux, *Science* **1994**, 263, 658.
- 2 M. Kurmoo, A. W. Graham, P. Day, S. J. Coles, M. B. Hursthouse, J. L. Caulfield, J. Singleton, J. P. Francis, W. Hayes, L. Ducasse, P. Guionneau, *J. Am. Chem. Soc.* **1995**, 117, 12209.
- 3 S. Ohkoshi, A. Fujishima, K. Hashimoto, *J. Am. Chem. Soc.* **1998**, 120, 5349.
- 4 *Magnetism: A Supramolecular Function*, ed. by O. Kahn, Kluwer Academic Publishers, **1996**.
- 5 E. Coronado, J. R. Galan-Mascaros, V. Laukhin, *Nature* **2000**, 408, 447.
- 6 K. Inoue, T. Hayamizu, H. Iwamura, D. Hashizume, Y. Ohashi, *J. Am. Chem. Soc.* **1996**, 118, 1803.
- 7 K. Inoue, H. Iwamura, *J. Am. Chem. Soc.* **1994**, 116, 3173.

- 8 H. Iwamura, K. Inoue, N. Koga, *New J. Chem.* **1998**, 22, 201.
- 9 A. S. Markosyan, T. Hayamizu, H. Iwamura, K. Inoue, *J. Phys.: Condens. Matter* **1998**, 10, 2323.
- 10 H. Kumagai, K. Inoue, *Angew. Chem., Int. Ed. Engl.* **1999**, 38, 1601.
- 11 L. D. Barron, J. Vrbancich, *Mol. Phys.* **1984**, 51, 715.
- 12 G. L. J. A. Rikken, E. Raupach, *Nature* **1997**, 390, 493.
- 13 P. Day, *Acc. Chem. Res.* **1979**, 12, 236.
- 14 A. Caneschi, D. Gatteschi, P. Rey, *Progress in Inorganic Chemistry*, ed. by S. J. Lippard, John Wiley & Sons, Inc., **1991**, Vol. 39, p. 331.
- 15 R. Feyerherm, A. Loose, T. Ishida, T. Nogami, J. Kreitlow, J. Baabe, F. J. Litterst, S. Sullow, H.-H. Klauss, *Phys. Rev. B* **2004**, 69, 1344427.
- 16 J. Seiden, *J. Phys. Lett.* **1983**, 44, 947.